Bidirectional Contactless Power Transfer System Expandable from Unidirectional System

Soichiro Nakadachi*, Shigeru Mochizuki*, Sho Sakaino*, Yasuyoshi Kaneko*, Shigeru Abe*, Tomio Yasuda**
*Saitama University, Saitama, Japan
**Technova Inc., Tokyo, Japan
S12mm235@mail.saitama-u.ac.jp

***Abstract*— Contactless power transfer (CPT) systems with primary series and secondary parallel capacitors (SP topology) are useful for charging electric vehicles. However, SP topology is not suitable for bidirectional power transfer. This paper introduces a novel SPL topology for bidirectional CPT systems that is realized by adding an inductor and an inverter to the SP topology. The 3kW and 160mm gap bidirectional test results show that the efficiency of G2V is 92.5%, and the efficiency of V2G is 93.4%, which are approximately equal to the efficiency of the unidirectional SP topology system of 93.1%.**

I. INTRODUCTION

The development and commercialization of plug-in hybrid electric vehicles (PHVs) and electric vehicles (EVs) are being actively pursued due to environmental concerns and rising oil prices. Both PHVs and EVs currently require a physical connection to power supplies by electric cables for battery charging.

In recent years, contactless power transfer (CPT) systems have been developed as a new battery charging method in which the battery can be charged simply by parking the cars in a predefined position. Although CPT systems have been researched extensively, most of these systems are unidirectional grid (home) to vehicle (G2V) power transfer systems [1-4].

Current charging methods using electric cables (with a focus on large EV batteries) have been researched extensively for use in bidirectional power transfer systems, which can also transfer power from the vehicle to the home (V2H or V2G). These systems use the EV batteries as energy storage for homes, movable power supplies, and emergency power supplies. Similarly, CPT systems should also accommodate bidirectional power transfer.

Madawalara *et al.* [5] proposed a point-to-multipoint bidirectional CPT system that allows for bidirectional power transfer by operating the primary and secondary inverters and controlling the phase between these inverters. They used a CPT system with primary parallel and secondary parallel capacitors (PP topology).

The other method for controlling the power is by operating only the transmitter side inverter and using the receiver side inverter as a rectifier. As for the capacitor topology, series and series capacitors (SS topology) [6, 7] and series and parallel capacitors (SP topology) are applicable.

The SS topology can easily transfer the power bidirectionally due to its symmetrical circuit. However, the SS topology has immittance converter characteristics [8]; that is, if the input voltage is constant, the output current is constant. This is not suited for keeping the battery voltage constant during the final stage of charging.

On the other hand, the SP topology has the ideal transformer characteristics: if the input voltage is constant, the output voltage is constant. This is suited for precise charge control of Li-ion batteries. Moreover, the secondary voltage of the transformer is kept low compared to that for the SS topology, since it is desirable to avoid high voltages inside a car. However, in V2G, the square voltage waveform of the inverter causes a problem: a large harmonic current flows into the parallel capacitor at the secondary side.

In this paper, we propose a novel SPL (SP plus L) topology that resolves this problem and has good characteristics. The SPL topology achieves bidirectional power transfer by adding an inductor (L_S) to the SP topology and by changing the C_S value slightly. The SPL topology allows bidirectional power transfer with high efficiency and simplifies the control of inverters by operating only one side of the inverter. The SPL topology also has an excellent feature where the primary and secondary voltages become equal between G2V and V2G if the same rated power is transferred at maximum efficiency. This means that the capacity (KVA) of the bidirectional system's inverter is almost equal to that of the unidirectional system's inverter and rectifier.

II. BIDIRECTIONAL CONTACTLESS POWER TRANSFER SYSTEM

A. System configuration

Figure 1(a) shows a schematic diagram of the conventional unidirectional CPT system using the SP

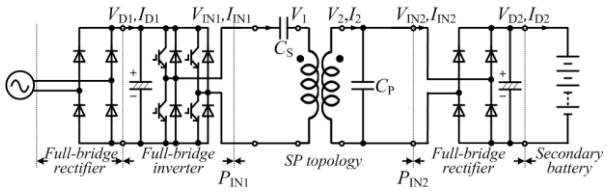

(a) Unidirectional CPT system

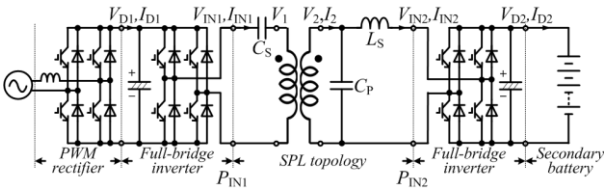

(b) Bidirectional CPT system

Figure 1. CPT systems.

topology. The 50Hz/60Hz AC power is converted to high-frequency 50kHz~150kHz AC power by the inverter at the primary side, transferred to the secondary side through a contactless power transformer, and then converted into DC power to charge the battery.

Figure 1(b) shows the proposed bidirectional CPT system using the SPL topology. The extension procedure is as follows:

- Change the rectifier in the primary side to a bidirectional PWM rectifier.
- Change the C_S value in the primary side slightly.
- Add an inductor (L_S) to the secondary side.
- Change the rectifier in the secondary side to an inverter.

The primary and secondary inverters can be used as rectifiers by turning all switching devices (e.g., IGBT and FET) off. By operating the transmitting side inverter as a normal inverter and the receiving side inverter as a rectifier, this system can control the power transfer direction.

B. SP topology (series and parallel resonant capacitor topology)

Figure 2 shows a detailed equivalent circuit for the SP topology. It consists of a T-shaped equivalent circuit in which the primary series capacitor C_S, the secondary parallel capacitor C_P, and a resistance load R_L have been added. The battery and rectifier located in the vehicle are approximated as R_L, whose value is determined as $R_L=V_{IN2}{}^2/P_L$, where V_{IN2} is the secondary voltage, and P_L is the secondary power. The primary values are converted into secondary equivalent values by a turn ratio ($a=N_1/N_2$) and are represented by the prime symbol. The winding resistances (r'_1 and r_2) and the ferrite core loss (r'_0) are considerably lower than the mutual and leakage reactance (x'_0, x'_1, and x_2) at the resonant frequency. Therefore, r'_1, r_2, and r'_0 can be omitted in the circuit for the analysis.

To achieve resonance with the self-reactance of the secondary winding $\omega_0 L_2$, which is equivalent to adding a

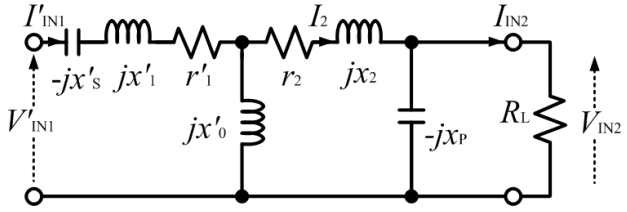

Figure 2. Equivalent circuit of SP topology.

mutual reactance x'_0 ($=\omega_0 l'_0$) and a leakage reactance x_2 ($=\omega_0 l_2$), the secondary parallel capacitor C_P is given by

$$\frac{1}{\omega_0 C_P} = \omega_0 L_2 = x_P = x'_0 + x_2 \tag{1}$$

The primary series capacitor C'_S ($= a^2 C_S$) is determined as

$$\frac{1}{\omega_0 C'_S} = x'_S = x'_1 + \frac{x'_0 x_2}{x'_0 + x_2} \tag{2}$$

The input-output characteristic of the SP topology can be expressed by the F matrix as

$$\begin{bmatrix} V_{IN1} \\ I_{IN1} \end{bmatrix} = \begin{bmatrix} ab & 0 \\ 0 & 1/ab \end{bmatrix} \begin{bmatrix} V_{IN2} \\ I_{IN2} \end{bmatrix} \quad \left(a = \frac{N_1}{N_2} \quad b = \frac{x'_0}{x'_0 + x_2} \right) \tag{3}$$

Equation (3) indicates that the equivalent circuit for a transformer with these capacitors is the same as an ideal transformer with a voltage ratio of ab at the resonant frequency. The b is almost equal to the coupling coefficient k of the contactless transformer. The voltage ratio between the primary and secondary sides (V_{IN2}/V_{IN1}) can be set to any value by selecting a ($=N_1/N_2$) corresponding to k. However, in the SP topology, V2G is not allowed because of the large harmonic current flowing through C_P.

C. SPL topology (series and parallel resonant capacitor plus L topology)

The SPL topology is a novel circuit topology that can be obtained by adding an inductor L_S to the SP topology and solves the issue of harmonic current. Figure 3 shows a detailed equivalent circuit for the SPL topology. The values of C_S and C_P are determined by (6) and (7) to achieve resonance with the self-reactance of the connected side winding.

$$\frac{1}{\omega_0 C'_S} = \omega_0 L'_1 = x'_S = x'_0 + x'_1 \tag{6}$$

$$\frac{1}{\omega_0 C_P} = \omega_0 L_2 = x_P = x'_0 + x_2 \tag{7}$$

Here, L_1 and L_2 are the self-inductances of the primary and secondary windings, respectively. Since (7) is the same as (1), the value of C_P does not need to be changed if it is used in the SPL topology. The value of the added inductor L_S is given by (8) to be the same value as L_2

$$L_S = L_2 \tag{8}$$

When C_S, C_P, and L_S are determined as (6)-(8), and the input-output characteristics of the SPL topology in G2V can be expressed by an F matrix as

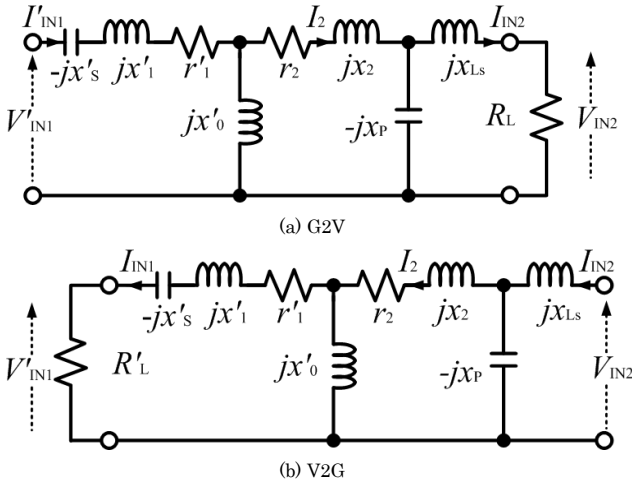

Figure 3. Equivalent circuit of SPL topology.

$$\begin{bmatrix} V_{IN1} \\ I_{IN1} \end{bmatrix} = \begin{bmatrix} ab & 0 \\ 0 & 1/ab \end{bmatrix} \begin{bmatrix} V_{IN2} \\ I_{IN2} \end{bmatrix} \quad \left(a = \frac{N_1}{N_2} \quad b = \frac{x'_0}{x'_0 + x_2} \right) \tag{9}$$

Equation (9) is the same as (3). Thus, the input-output characteristics of the SPL and SP topologies are expressed by the same F matrix, which is equivalent to an ideal transformer with a voltage ratio of *ab*.

D. Condition for maximum efficiency operation

In the SPL topology, R_L should be appropriately selected to operate at maximum efficiency. The efficiency of the contactless power transformer η_{G2V} (=P_{IN2}/P_{IN1}) is expressed by equation (9) because r_0 is sufficiently smaller than r_1 and r_2 to be ignored in this analysis.

$$\eta_{G2V} = \frac{R_L I_{IN2}^2}{r'_1 I'^2_{IN1} + r_2 I_2^2 + R_L I_{IN2}^2} \tag{11}$$

Here, the resistance of inductor (*Ls*) is ignored as well. The relationship between V_2, I_2, V_{IN2}, and I_{IN2} is given by

$$\begin{bmatrix} V_2 \\ I_2 \end{bmatrix} = \begin{bmatrix} 1 & j(x'_0 + x_2) \\ j\dfrac{1}{x'_0 + x_2} & 0 \end{bmatrix} \begin{bmatrix} V_{IN2} \\ I_{IN2} \end{bmatrix} \tag{12}$$

Equation (12) can also be expressed as

$$I_2 = j\frac{V_{IN2}}{x'_0 + x_2} = j\frac{I_{IN2} R_L}{x'_0 + x_2} \quad , \quad \left| \frac{I_2}{I_{IN2}} \right|^2 = \left(\frac{R_L}{x'_0 + x_2} \right)^2 \tag{13}$$

Equation (14) is obtained by substituting $I'_{IN1}=I_{IN2}/b$ developed from (9) and (13) into (11).

$$\eta_{G2V} = \frac{R_L}{R_L + r_2 \dfrac{R_L^2}{(x'_0 + x_2)^2} + \dfrac{r'_1}{b^2}} \tag{14}$$

Equation (14) shows that η_{G2V} depends on the value of R_L. The maximum efficiency in G2V (η_{maxG2V}) is obtained when $R_L=R_{LmaxG2V}$ is expressed by

$$\eta_{max\,G2V} = \frac{1}{1 + \dfrac{2}{x'_0}\sqrt{r'_1 r_2}} \tag{15}$$

$R_{LmaxG2V}$ is given by

$$R_{L\max G2V} = \frac{(x'_0 + x_2)^2}{x'_0} \sqrt{\frac{r'_1}{r_2}} \tag{16}$$

Similarly, in V2G, the efficiency of the contactless power transformer η_{V2G} (=P_{IN1}/P_{IN2}) is expressed by

$$\eta_{V2G} = \frac{R'_L I'^2_{IN1}}{r'_1 I'^2_{IN1} + r_2 I_2^2 + R'_L I'^2_{IN1}} \tag{17}$$

The relationship between V_2, I_2, V_{IN2}, and I_{IN2} is given by

$$\begin{bmatrix} V_2 \\ I_2 \end{bmatrix} = \begin{bmatrix} \dfrac{x'_0 + x_2}{x'_0} & -jx'_0 \\ -j\dfrac{1}{x'_0} & 0 \end{bmatrix} \begin{bmatrix} V'_{IN1} \\ I'_{IN1} \end{bmatrix} \tag{18}$$

Equation (18) can also be expressed as

$$I_2 = -j\frac{V'_{IN1}}{x'_0} = -j\frac{I'_{IN1} R'_L}{x'_0}, \quad \left| \frac{I_2}{I'_{IN1}} \right|^2 = \left(\frac{R'_L}{x'_0} \right)^2 \tag{19}$$

Then, equation (20) is obtained by substituting (19) into (17).

$$\eta_{V2G} = \frac{R'_L}{R'_L + r'_1 + r_2 \left(\dfrac{R'_L}{x'_0} \right)^2} \tag{20}$$

Thus, the maximum efficiency in V2G (η_{maxV2G}) and the value of $R_{LmaxV2G}$, which maximizes η_{V2G}, are expressed by

$$\eta_{max\,V2G} = \frac{1}{1 + \dfrac{2}{x'_0}\sqrt{r'_1 r_2}} \tag{21}$$

$$R'_{L\max V2G} = \frac{1}{a^2} R_{L\max V2G} = x'_0 \sqrt{\frac{r'_1}{r_2}} \tag{22}$$

In the case of G2V, the value of R_L should be selected as $R_L= R_{LmaxG2V}$ from equation (16), and in the case of V2G, the value of R_L should be selected as $R_L= R_{LmaxV2G}$ from equation (22). Since the value of R_L is also determined by the load voltage V_L and the load power P_L as $R_L=V_L^2/P_L$, the transformer is usually designed to be $R_{Lmax}=R_L=V_L^2/P_L$. In the case of a bidirectional system, it is desirable that $R_{LmaxG2V}$ and $R_{LmaxV2G}$ have the almost same value.

E. Power characteristic at maximum efficiency operation in both G2V and V2G

The bidirectional CPT system requires high efficiency and a comparable voltage level in both power directions (G2V and V2G). In the following, we present the relationship between the output power, the primary voltage (V_{IN1}), and the secondary voltage (V_{IN2}) at the maximum efficiency.

Equations (15) and (16) can be expressed by (24) and (25) using *k* and *Q* as defined in (23).

$$k = \frac{M}{\sqrt{L_1 L_2}}, \quad Q_1 = \frac{\omega_0 L_1}{r_1}, \quad Q_2 = \frac{\omega_0 L_2}{r_2} \tag{23}$$

$$\eta_{max\,G2V} = \frac{1}{1 + \dfrac{2}{k}\sqrt{\dfrac{1}{Q_1 Q_2}}} \tag{24}$$

TABLE I. R_{Lmax} AND $\eta_{\max}$ OF EACH TOPOLOGY

	SP(G2V)	SPL(G2V)	SPL(V2G)
R_{Lmax}	$\left(x_0'+x_2\right)\sqrt{\frac{1}{b^2}\frac{r_1'}{r_2}+1}$	$\frac{\left(x_0'+x_2\right)^2}{x_0'}\sqrt{\frac{r_1'}{r_2}}$	$a^2x_0'\sqrt{\frac{r_1'}{r_2}}$
$\eta_{\max}$	$\frac{1}{1+\frac{2r_2}{x_0'+x_2}\sqrt{\frac{1}{b^2}\frac{r_1'}{r_2}+1}}$	$\frac{1}{1+\frac{2}{x_0'}\sqrt{r_1'r_2}}$	$\frac{1}{1+\frac{2}{x_0'}\sqrt{r_1'r_2}}$
$R_{\mathrm{Lmax\ Q}}$	$\frac{r_2Q_2}{k}\sqrt{\frac{Q_2}{Q_1}}$	$\frac{r_2Q_2}{k}\sqrt{\frac{Q_2}{Q_1}}$	$a^2kr_1'\sqrt{Q_1Q_2}$
$\eta_{\max\ Q}$	$\frac{1}{1+\frac{2}{k}\sqrt{\frac{1}{Q_1Q_2}}}$	$\frac{1}{1+\frac{2}{k}\sqrt{\frac{1}{Q_1Q_2}}}$	$\frac{1}{1+\frac{2}{k}\sqrt{\frac{1}{Q_1Q_2}}}$

$$R_{L\max G2V}=\frac{r_2Q_2}{k}\sqrt{\frac{Q_2}{Q_1}} \tag{25}$$

Similarly, in V2G, (21) and (22) can be expressed by (26) and (27),

$$\eta_{\max V2G}=\frac{1}{1+\frac{2}{k}\sqrt{\frac{1}{Q_1Q_2}}} \tag{26}$$

$$R'_{L\max V2G}=kr_1'\sqrt{Q_1Q_2} \tag{27}$$

where $r'_1=r_1/a^2$.

Considering (16) and (22), the relationship between R_{LmaxG2V} and R_{LmaxV2G} is given by

$$R_{L\max G2V}=\frac{1}{b^2}x_0'\sqrt{\frac{r_1'}{r_2}}=\frac{R'_{L\max V2G}}{b^2}=\frac{R_{L\max V2G}}{a^2b^2}. \tag{28}$$

When the efficiency is maximum in G2V, the secondary voltage $V_{\mathrm{IN2(G2V)}}$, the output power P_{G2V} (=P_{IN2}), and R_{LmaxG2V} satisfy the following relationship:

$$R_{L\max G2V}=V^2_{\mathrm{IN2(G2V)}}/P_{\mathrm{G2V}}. \tag{29}$$

On the other hand, the equivalent resistance in V2G with the output power P_{V2G} (=P_{IN1}) in G2V is expressed as follows:

$$R_{LV2G}=V^2_{IN1}/P_{V2G}=\left(abV^2_{IN2}\right)/P_{V2G} \tag{30}$$

For the case in which P_{V2G} = P_{G2V} and V_{IN2} = $V_{\mathrm{IN2(G2V)}}$, R_{LG2V} is derived as follows:

$$R_{LG2V}=\frac{\left(abV_{IN2(G2V)}\right)^2}{P_{V2G}}=(ab)^2R_{L\max G2V}=R_{L\max V2G} \tag{31}$$

Equation (31) shows that the primary and secondary voltages do not change between G2V and V2G if the same rated power is transferred at maximum efficiency. This is an excellent feature of the SPL topology and means that the capacity (KVA) of the bidirectional system's inverter is almost equal to the capacity of the unidirectional system's inverter and rectifier.

R_{LmaxQ} and η_{maxQ} in each direction expressed using k and Q are shown in Table I. The values of η_{maxQ} are found to be equal in the two topologies (SP and SPL). Note that the approximation expressed by equation (32) is used to calculate R_{LmaxQ} and η_{maxQ} for the SP topology.

$$\frac{1}{k^2}\frac{Q_2}{Q_1}>>1 \tag{32}$$

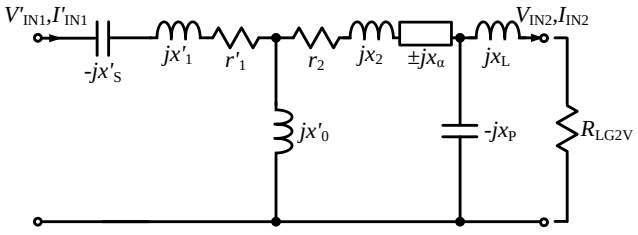

Figure 4. Regulation of voltage ratio added reactance.

F. *Adjustment of the secondary voltage by inserting C and L*

The voltage ratio ($V_{\mathrm{IN1}}/V_{\mathrm{IN2}}$) can be adjusted easily by changing the self-inductance of the secondary winding L_2. This means that the voltage ratio can be adjusted by inserting C or L between the secondary winding and C_{P}. Figure 4 shows a detailed equivalent circuit for the SPL topology when C or L are inserted. Here, x_α is the reactance of C or L. When the values of C_{P} and L_{S} are determined as (33), the input-output characteristics $\eta_{\max}$ and R_{Lmax} in each direction can be expressed by (34)-(37)

$$\frac{1}{\omega_0C_P}=\omega_0L_S=x_P=x_L=x_0'+x_2\pm x_\alpha \tag{33}$$

$$\begin{bmatrix}V_{IN1}\\I_{IN1}\end{bmatrix}=\begin{bmatrix}\frac{ab}{c} & 0\\ 0 & \frac{c}{ab}\end{bmatrix}\begin{bmatrix}V_{IN2}\\I_{IN2}\end{bmatrix} \tag{34}$$

$$\eta_{\max G2V}=\eta_{\max V2G}=\frac{1}{1+\frac{2}{x_0'}\sqrt{r_1'r_2}} \tag{35}$$

$$R_{L\max G2V}=\frac{c^2\left(x_0'+x_2\right)^2}{x_0'}\sqrt{\frac{r_1'}{r_2}},\quad R'_{L\max V2G}=x_0'\sqrt{\frac{r_1'}{r_2}} \tag{36}$$

$$c=\frac{x_0'+x_2\pm x_\alpha}{x_0'+x_2} \tag{37}$$

Here, c is the step up or step down ratio defined by (37). When L is inserted to increase L_2, x_α is positive. On the other hand, when C is inserted to decrease L_2, x_α is negative. Equations (34)-(37) show that the voltage ratio ($V_{\mathrm{IN1}}/V_{\mathrm{IN2}}$) can be also changed by c. In addition, $\eta_{\max}$ does not change based on whether L or C is inserted.

III. EXPERIMENTAL RESULTS

In order to verify the performance of the proposed SPL topology, a 3kW bidirectional CPT test was conducted. In addition, a 3kW unidirectional CPT test with the SP topology was also carried out to compare its performance with that of the SPL topology. In the test, the inverter frequency was 50kHz, and the value of R_{L} was selected to

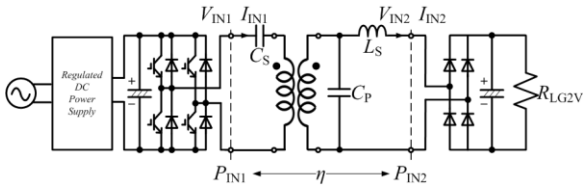

(a) G2V

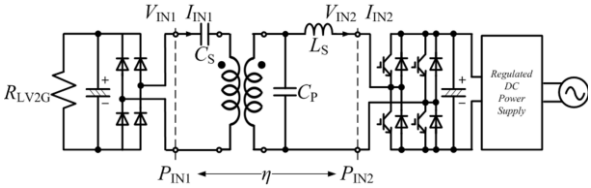

(b) V2G

Figure 5. Experimental circuit.

Figure 6. Photgraph of transformer.

TABLE II. PARAMETERS OF TRANSFORMER

Freq [kHz]	50	L_1 [μH]	144.8
Gap [mm]	160	L_2 [μH]	6.0
N_1	20	C_S [μF]	0.070
N_2	4	C_P [μF]	1.697
k	0.170	L_S [μH]	6.0

maximize the efficiency in the SPL (G2V and V2G) and SP topologies.

A. *A contactless power transformer and experimental circuit*

Figure 5 shows the experimental circuits for each direction (G2V and V2G). Figure 6 shows the 3kW transformer used in the bidirectional CPT test [9]. Table II shows the transformer parameters at the normal position (a gap length of 160mm and no misalignment).

B. *Characteristics of normal position*

First, the result of the 3kW bidirectional CPT test in the normal position is described. The test condition was a gap length of 160mm with no misalignment. The test results are shown in Table III and Figure 7. Table III shows the test results for the SP's G2V, the SPL's G2V, and V2G. The efficiency in the SPL topology (η_{G2V} or η_{V2G}) was approximately 93% when the output power was 3 kW, which is nearly equal to the SP topology (η_{SP}) efficiency of 93.1%. The reason why the efficiency of V2G was higher than the

TABLE III. EXPERIMENTAL RESULTS

(NORMAL POSITION)

	G2V	V2G	SP(G2V)
R_L [Ω]	17.5	10	15
R_{Lmax} [Ω]	10.9	8.0	12.9
V_{IN1} [V]	201.6	173.1	184.1
V_{IN2} [V]	202.5	193.5	183.2
V_{IN2}/V_{IN1}	1.00	1.12	1.00
P_{IN1} [W]	3319	3067	3314
P_{IN2} [W]	3069	3284	3084
η [%]	92.5	93.4	93.1
η_{max} [%]	97.1	97.1	97.1

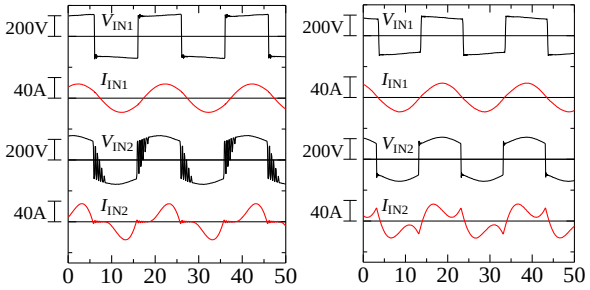

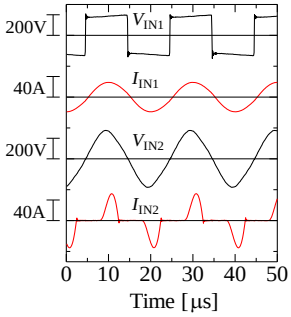

(c) SP topology (G2V)

Figure 7. Experimental waveform of SPL topology.

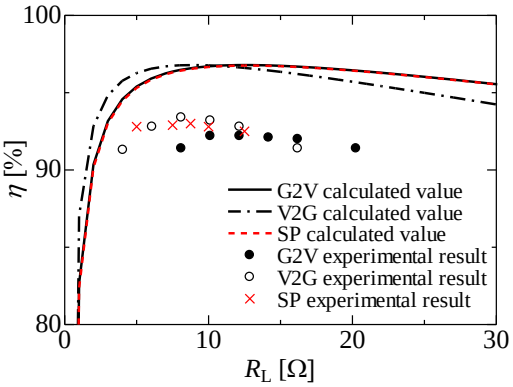

Figure 8. Transformer efficiency with load change.

TABLE IV. EXPERIMENTAL RESULTS WITH CHANGE IN POSITION AND AIR GAP

position										
	x [mm]	0		100		0		0		0	
	y [mm]	0		0		200		0		0	
	gap [mm]	160		160		160		120		200	
direction		G2V	V2G	G2V	V2G	G2V	V2G	G2V	V2G	G2V	V2G
R_L [Ω]		17.5	10	17.5	10	17.5	10	17.5	10	17.5	10
V_{IN1} [V]		201.6	173.1	154.7	173.5	139.2	173.7	285.6	173.7	148.9	173.7
V_{IN2} [V]		202.5	193.5	202.5	313.6	202.7	299	202.3	135.2	202.5	267.4
V_{IN2}/V_{IN1}		1.00	1.12	1.31	1.81	1.46	1.72	0.71	0.78	1.36	1.54
P_{IN1} [W]		3319	3067	3430	3067	3499	3068	3257	3068	3453	3068
P_{IN2} [W]		3069	3284	3067	3483	3071	3455	3070	3232	3071	3401
η [%]		92.5	93.4	89.4	88.0	87.8	88.8	94.2	94.9	88.9	90.2

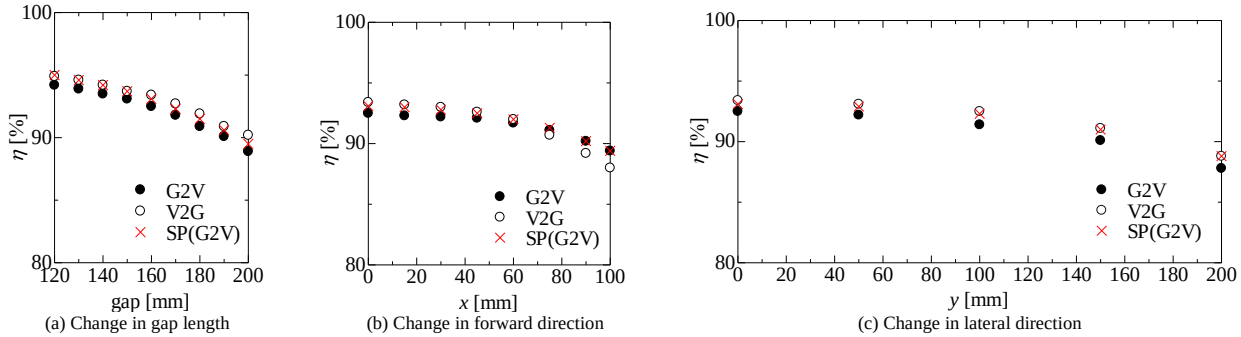

(a) Change in gap length (b) Change in forward direction (c) Change in lateral direction

Figure 9. Efficiency with change in position and air gap.

efficiency of the SP topology is considered to be measurement error.

Figure 7 shows the input and output voltage and current. The primary and secondary voltages were almost coherent, which demonstrates that the SPL topology has the characteristics of an ideal transformer in both directions. In Figure 7(a), there are LC oscillations around the instances of voltage switching. This oscillation appears when the current I_{IN2} becomes discontinuous.

C. *Characteristics with resistance-load change*

Figure 8 shows the experimental efficiency when R_L is changed and the curves of calculated value are derived from (14) and (20). Here, the value of R_L is calculated from the input voltage V_{IN1}, V_{IN2} of the full-bridge rectifier and the power running through it. Since the theoretical efficiency ignores the core loss, the theoretical efficiencies are higher than the experimental efficiencies, and the difference corresponds to the core loss. Both efficiencies show the same characteristics.

During battery charging, the battery voltage is almost constant. Therefore, Figure 8 represents the change in efficiency when the charging power is changed.

D. *Characteristics with change in gap length and misalignment*

In the contactless power transfer system for EVs, misalignment of the transformer due to the driver's skill and the change in the gap length from the car's weight is inevitable. The coupling factor k depends on the relative position between the primary and secondary transformers, and the efficiency decreases with a decrease in k.

Table IV shows the test results when a change in gap length and forward / lateral misalignment occurred. Here, x is the forward direction, and y is the lateral direction of the car.

Figure 9 shows the efficiency when the gap length and misalignment are changed. The efficiency of the SPL topology is almost the same as that of the SP topology

E. *Frequency characteristics of SPL topology*

Because CPT systems have a resonance circuit, it is necessary to know the characteristics of the circuit when the inverter frequency is changed. Figure 10 shows the frequency characteristics of the impedance of the SPL circuit with load from the output terminal of the inverter. Here, the impedance is calculated from the measured parameters of the transformer. If the frequency is changed in the range of ±2% (±1kHz), the absolute value of the impedance changes slightly in both G2V and V2G.

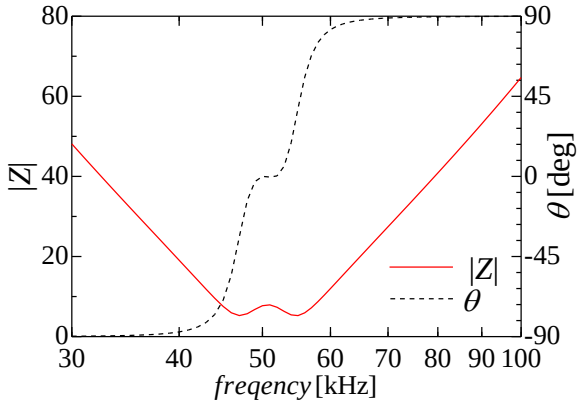

(a) G2V

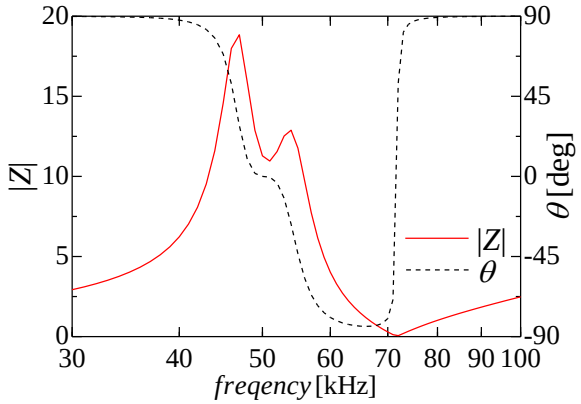

(b) V2G

Figure 10. Frequency characteristics of Z

IV. CONCLUSION

We proposed a novel SPL topology for a bidirectional contactless power transfer system. The SPL topology is expandable from the SP topology by adding an inductor to the secondary side, changing the primary capacitor value, and replacing the secondary rectifier with an inverter.

The input / output characteristics of the SPL topology are equal to those of an ideal transformer with a turn ratio of *b* for the SP topology. The power transfer control enables bidirectional power transfer (G2V and V2G) with high efficiency at the rated power.

The 3kW bidirectional test results show that the efficiency of the SPL topology in G2V is 92.5%, and the efficiency of the SPL topology in V2G is 93.4%, which are approximately equal to the efficiency of the unidirectional SP topology of 93.1%.

The proposed SPL topology can be used not only for vehicles but also for other CPT systems. We hope that this will allow a wider range of applications of bidirectional CPT technology.

REFERENCES

[1] Yuichi Nagatsuka, N. Ehara, Y. Kaneko, S. Abe, and T. Yasuda "Compact Contactless Power Transfer System for Electric Vehicles" IPEC2010-Sapporo pp. 807-813(2010)

[2] M. Chigira, Y. Nagatsuka, Y. Kaneko, S. Abe, T. Yasuda, and A.Suzuki "Small-Size Light-Weight Transformer with New Core Structure for Contactless Electric Vehicle Power Transfer System" ECCE2011-PHOENIX pp. 260-266(2011)

[3] M. Budhia, G. Covic, and J. Boys "Development of a Single-Sided Flux Magnetic Coupler for Electric Vehicle IPT Charging Systems", *IEEE Trans. Ind. Electron*., Vol. 60, No. 1, January 2013, pp. 318-328

[4] G. Covic and J. Boys, "Inductive Power Transfer", *Proc IEEE*, Vol. 101, No. 6, June 2013, pp. 1276-1289

[5] U. K. Madawala and D. J. Thrimawithana, "A Bidirectional Inductive Power Interface for Electric Vehicles in V2G Systems", *IEEE Trans. Ind. Electron*., Vol. 58, No. 10, pp. 4789-4796 (2011)

[6] C.-S. Wang, G. Covic, and O. H. Stielau "General Stability Criterions for Zero Phase Angle Controlled Loosely Coupled Inductive Power Transfer Systems" in *Proc. IEEE IECON'01*, vol. 2, 2001, pp. 1049-1054.

[7] Y. Jang, and M. M.Jovanovic "A Contactless Electrical Energy Transmissin System for Portable- Telephone Battery Chargers" *IEEE Trans. Ind. Electron*., Vol. 50, No. 3, June 2003, pp. 520-527

[8] H. Irie, and T. Yabuuchi "High-Frequency Constant-Current Power Supply in Noncontact Energy Transfer System Using Immittance Conver" Electrical Engineering in Japan, Vol. 158, No. 3, 2007, pp. 81-89

[9] H.Takanashi, Y. Kaneko, S. Abe, and T.Yasuda "A Large Air Gap 3 kW Wireless Power Transfer System for Electric Vehicles" ECCE2012, North Carolina, pp.269-274 (Sep 15-20 2012)